J. Fluid Mech. (2023), *vol*. 965, R1, doi:10.1017/jfm.2023.372

Viscous damping of steady-state resonant sloshing in a clean rectangular tank

Anton Miliaiev[1] **and Alexander Timokha**[1],†

[1]Institute of Mathematics of the National Academy of Sciences of Ukraine, 01024 Kyiv, Ukraine

(Received 16 February 2023; revised 30 April 2023; accepted 30 April 2023)

A machine learning of the unknown *a priori* viscous damping, incorporated into the single-dominant nonlinear 'inviscid' modal theory by Faltinsen *et al.* (*J. Fluid Mech.*, vol. 407, 2000, pp. 201–234) on resonant sloshing (the forcing frequency close to the lowest natural sloshing frequency) in a clean (no internal structures) rigid rectangular tank, is proposed. The learning procedure requires a set of measured phase lags between the harmonic horizontal tank excitation and the steady-state resonant wave response. A good consistency with experiments by Bäuerlein & Avila (*J. Fluid Mech.*, vol. 925, 2021, A22) on the liquid-mass centre motions is shown. The latter confirms that the free-surface nonlinearity (causing an energy flow from the primary-excited to higher natural sloshing modes) and viscous damping of the higher natural sloshing modes matter, as well as that the damping rates can depend on the steady-state wave amplitude.

Key words: interfacial flows (free surface)

1. Introduction

When a clean rigid rectangular tank with a finite liquid depth is longitudinally excited with the forcing frequency close to the lowest natural sloshing frequency, the free-surface nonlinearity causes an energy flow (Faltinsen & Timokha 2009; Pilipchuk 2013) from the lowest (primary-excited) to higher natural sloshing modes so that the nonlinearity becomes a prevailing mechanism preventing an infinite resonant wave-amplitude response. Viscous damping plays then a secondary role (Faltinsen & Timokha 2001). This explains why the single-dominant (applicable for smaller excitation amplitudes, Faltinsen *et al.* 2000) and adaptive (it should be adopted with increasing the forcing amplitude and at the critical liquid depth, Faltinsen & Timokha 2001) 'inviscid' weakly nonlinear modal theories/systems provide satisfactory agreement with the measured steady-state wave-amplitude characteristics. However, these theories fail to predict the phase-lag response curve, which is, theoretically, piecewise (the phase lag possesses the values 0 and

† Email address for correspondence: atimokha@gmail.com

$\pm\pi$) in the inviscid approximation while accounting for damping makes it continuous. The phase-lag response is most sensitive to the damping in those mechanical systems. Hence, having known a set of measured phase lags and introducing physically and mathematically consistent unknown *a priori* damping terms in the modal systems, one could implement (according to the so-called hidden-physics concept by Raissi & Karniadakis 2018; Raissi, Perdikaris & Karniadakis 2019; Ahmed *et al.* 2021), as discussed by Ahmed *et al.* (2021) for the reduced order modelling as well as by Saltari *et al.* (2022) for violent liquid sloshing due to vertical excitations, a machine learning procedure to implicitly deduce the introduced viscous damping terms.

Appropriate measurements of the phase lag were recently reported by Bäuerlein & Avila (2021) who utilised them to evaluate a constant damping ratio in the Duffing equation, which was adopted by the authors as a phenomenological mathematical model of horizontal motions of the liquid-mass centre (spring and pendulum-type phenomenological models are often employed for sloshing: see Miles 1962; NASA 1968; Aliabadi, Johnson & Abedi 2003; Godderidge, Turnock & Tan 2012, and references therein). This damping ratio, ξ, had to equal 15×10^{-3} to more or less satisfactory approximate the experimental data. Using the same experimental set-up, Bäuerlein & Avila (2021) analysed logarithmic decrements of the first (lowest) natural sloshing mode and, thereby, computed its damping ratio $\xi_1^{exp} = 8.4 \times 10^{-3}$. This experimental value is larger than its theoretical prediction ($\xi_1^{(0)} = 5.7 \times 10^{-3}$) by Keulegan (1959). Because the first differential equation of the single-dominant nonlinear modal system by Faltinsen *et al.* (2000) governs perturbations of the first natural sloshing mode, Bäuerlein & Avila (2021) inserted the linear damping term with ξ_1^{exp} into this equation, derived a steady-state wave (periodic) solution, and showed that even in that case, the single-dominant modal theory is not able to satisfactory fit the measured steady-state resonant response.

A way of getting an excellent agreement is a purely data-driven (phenomenological) modelling dealing with dynamical systems with respect to amplitude and phase-lag parameters as it is demonstrated by Cenedese *et al.* (2022) exploiting the Stuart–Landau-type equation. Another way consists of following the hidden-physics concept suggesting a machine learning of physics-based dynamical models (ROMs) on sloshing derived from the original free-surface boundary problem. In the present paper, we step the second way. The single-dominant inviscid modal system by Faltinsen *et al.* (2000) is modified by incorporating the theoretically consistent damping terms. Implementing Moiseev's asymptotic scheme, a periodic (steady-state) solution of the modified system is derived, which, as the derivations show, depends on three unknown *a priori* parameters associated with the introduced damping. One parameter is responsible for the constant damping ratio of the second (-order) generalised coordinate (mode) but the other two are coefficients in the linear regression (by the dominant non-dimensional steady-state wave amplitude) chosen as the amplitude-dependent damping ratio for the first (lowest-order) generalised coordinate (mode). After defining the loss function as an integral distance between experimental (measured) and theoretical phase-lag curves, the gradient descent is applied to compute the three damping-related parameters. How it works is demonstrated with experimental phase lags by Bäuerlein & Avila (2021). An excellent agreement is shown except for the cases when, according to observations by Bäuerlein & Avila (2021), applicability of the single-dominant modal theory is questionable. Discrepancy between the linear damping quantities predicted by Keulegan (1959), coming from direct measurements by Bäuerlein & Avila (2021), and following from the present machine learning procedure is extensively discussed.

2. Single-dominant modal theory

We consider two-dimensional sloshing of an ideal liquid with irrotational flows in a rectangular tank of the width L and breadth B. The non-dimensional hydrodynamic statement suggests that L is the characteristic size and $T = 2\pi/\sigma_1$ is the characteristic time, where σ_1 is the lowest natural sloshing frequency. The tank is filled to a finite liquid depth which means that the non-dimensional (L-scaled) depth $h \gtrsim 0.4$ (Faltinsen & Timokha 2009, chap. 8). The tank oscillates harmonically with the forcing frequency σ close to σ_1. Based on rigorous mathematical results by Faltinsen (1974) and Ockendon & Ockendon (1973) concerning the steady-state resonant sloshing in a rectangular tank with a finite liquid depth (§ 8.2.2 in the textbook by Faltinsen & Timokha 2009), Faltinsen *et al.* (2000) proved that, if the non-dimensional forcing amplitude is relatively small, the nonlinear resonant sloshing, both steady-state and transient, can be described by employing the so-called single-dominant nonlinear modal system whose hydrodynamic generalised coordinates obligatory satisfy specific asymptotic relations in terms of the forcing amplitude. After inserting the framed viscous damping terms, the system takes the following non-dimensional form:

$$\ddot{\beta}_1 + \beta_1 + \boxed{2\xi_1[\dot{\beta}_1 + \Xi_1(\beta_m, \dot{\beta}_m|_{m=1,2})]} + d_1(\ddot{\beta}_1\beta_2 + \dot{\beta}_1\beta_2) + d_2(\ddot{\beta}_1\beta_1^2 + \dot{\beta}_1^2\beta_1) + d_3\ddot{\beta}_1\beta_1 = P_1\eta_{2a}\bar{\sigma}^2\cos(\bar{\sigma}t - \theta), \tag{2.1a}$$

$$\ddot{\beta}_2 + \bar{\sigma}_2^2\beta_2 + \boxed{2\bar{\sigma}_2\xi_2[\dot{\beta}_2 + \Xi_2(\beta_m, \dot{\beta}_m|_{m=1,2})]} + d_4\ddot{\beta}_1\beta_1 + d_5\dot{\beta}_1^2 = 0, \tag{2.1b}$$

$$\ddot{\beta}_3 + \bar{\sigma}_2^2\beta_3 + \boxed{2\bar{\sigma}_3\xi_3[\dot{\beta}_3 + \Xi_3(\beta_m, \dot{\beta}_m|_{m=1,2})]} + q_1\ddot{\beta}_1\beta_2 + q_2\ddot{\beta}_1\beta_1^2 + q_3\ddot{\beta}_2\beta_1 + q_4\dot{\beta}_1^2\beta_1 + q_5\dot{\beta}_1\dot{\beta}_2 = P_3\eta_{2a}\bar{\sigma}^2\cos(\bar{\sigma}t - \theta), \tag{2.1c}$$

$$\ddot{\beta}_m + \bar{\sigma}_m^2\beta_m + \boxed{2\bar{\sigma}_m\xi_m\dot{\beta}_m} = P_m\eta_{2a}\bar{\sigma}^2\cos(\bar{\sigma}t - \theta), \quad m \geqslant 4, \tag{2.1d}$$

where the hydrodynamic generalised coordinates $\beta_m(t)$ come from the functional (modal) representation of the free surface and necessarily fulfil the aforementioned Moiseev's asymptotic relations proven by Faltinsen (1974) and Ockendon & Ockendon (1973) (see also § 8.2.2 by Faltinsen & Timokha 2009),

$$z = \zeta(y, t) = \sum_{m=1}^{\infty} \beta_m(t)\cos\left(\pi m\left(y + \frac{1}{2}\right)\right), \tag{2.2a}$$

$$\beta_1 = O(\epsilon^{1/3}); \quad \beta_2 = O(\epsilon^{2/3}); \quad \beta_3 = O(\epsilon); \quad \beta_n \lesssim O(\epsilon), \quad n \geqslant 4; \quad P_1\eta_{2a} = \epsilon \ll 1, \tag{2.2b}$$

respectively. Here, σ_m are the natural sloshing frequencies, $\bar{\sigma} = \sigma/\sigma_1$, $P_m = 2/(\pi m)\tanh(\pi m h)((-1)^m - 1)$, $\bar{\sigma}_m^2 = \sigma_m^2/\sigma_1^2 = m\tanh(\pi m h)/\tanh(\pi h)$, the hydrodynamic coefficients d_n, q_n depend on the non-dimensional liquid depth h, $\eta_{2a} = O(\epsilon) \ll 1$ is the non-dimensional forcing amplitude, and θ is the phase lag in the external horizontal harmonic forcing. The computed values of the hydrodynamic coefficients are tabled by Faltinsen & Timokha (2009, chap. 9). A novelty with respect to the original work by Faltinsen *et al.* (2000) is the framed damping terms which we do not know *a priori*. As notified by Faltinsen & Timokha (2009, § 7.4), applicability of modal theories implicitly assumes a low-viscous liquid, i.e. the incorporated damping terms should be relatively small. What does it mean in the present paper is discussed below.

Because (2.1) is based on the Moiseev-type asymptotic relations (2.2*b*) with neglecting the $o(\epsilon)$-order quantities, only β_1 and β_2 are nonlinearly coupled (there is an energy flow between these two lower natural sloshing modes); β_3 is the 'driven' generalised hydrodynamic coordinate of the highest asymptotic order $O(\epsilon)$ but the natural sloshing modes with $m \geqslant 4$ are considered within the framework of the linear sloshing theory.

The same asymptotic relations should be true for the incorporated damping terms, that is, Ξ_i are only nonlinear functions of β_1 and β_2 and their first derivatives. Furthermore, in the linear limit with $\eta_{2a} = 0$ (free oscillations), the linear damping ratios ξ_i can be associated with logarithmic decrements of the natural sloshing modes $\cos(\pi i(y + \frac{1}{2}))$ in (2.2*a*). These ratios should be small for low-viscous liquids and, because our nonlinear analysis will centre around the two nonlinearly coupled generalised coordinates, β_1 and β_2, one can assume, as the 'most worse' case, that $\xi_1 \sim \xi_2$ possess the lowest asymptotic order $O(\epsilon^{1/3})$. Finally, because the asymptotic modal theory neglects the $o(\epsilon)$-order contribution in (2.1), one concludes $\Xi_3 = \Xi_2 = 0$ but $\Xi_1 = \Xi_1(\beta_1, \dot{\beta}_1)$ is a quadratic function, which we do not know *a priori* as well as ξ_i.

The steady-state resonant sloshing is associated with periodic solutions of (2.1). Following Moiseev's asymptotic scheme (Faltinsen & Timokha 2009, chap. 8), one can find an asymptotic approximation of these solutions even if (2.1) is equipped with the framed damping terms. In Moiseev's approximation, the lowest-order generalised hydrodynamic coordinates β_1 and β_2 take the form

$$\beta_1(t) = a\cos(\bar{\sigma}t) + O(a^3), \quad \beta_2(t) = a^2[l_0 + l_1\cos(2\bar{\sigma}t) + l_2\sin(2\bar{\sigma}t)] + O(a^4), \tag{2.3a,b}$$

where $a = O(\epsilon^{1/3}) > 0$ is the dominant (lowest-order) wave amplitude,

$$l_0 = \frac{d_4 - d_5}{2\bar{\sigma}_2^2}, \quad l_1(\xi_2) = \frac{(d_4 + d_5)(\bar{\sigma}_2 - 4)}{2((\bar{\sigma}_2^2 - 4)^2 + 16\bar{\sigma}_2^2\xi_2^2)}, \quad l_2(\xi_2) = \frac{2(d_4 + d_5)\bar{\sigma}_2\xi_2}{(\bar{\sigma}_2^2 - 4)^2 + 16\bar{\sigma}_2^2\xi_2^2}; \tag{2.4a–c}$$

the amplitude $a > 0$ and the phase lag θ come from the so-called secular system

$$a(m_1(\xi_2)a^2 + \hat{\sigma}^2 - 1) = \epsilon\cos\theta, \quad a(m_2(\xi_2)a^2 - 2\xi_1[1 + \xi a]) = \epsilon\sin\theta, \tag{2.5a,b}$$

which is derived after substituting (2.3*a*,*b*) into (2.1*a*) and collecting all quantities at $\cos(\bar{\sigma}t)$ and $\sin(\bar{\sigma}t)$ after applying the cosine angle-difference identity in the right-hand side and dividing by $\bar{\sigma}^2$; here,

$$m_1(\xi_2) = -\tfrac{1}{2}d_2 - 2d_3l_1 + d_1(-l_0 + \tfrac{1}{2}l_1), \quad m_2(\xi_2) = \tfrac{1}{2}l_2(d_1 - 4d_3), \quad \hat{\sigma} = \bar{\sigma}^{-1} \tag{2.6a–c}$$

and

$$\xi = -\frac{\bar{\sigma}}{\pi}\int_0^{2\pi/\bar{\sigma}} \Xi_1(\cos(\bar{\sigma}t), -\sin(\bar{\sigma}t))\sin(\bar{\sigma}t)\,\mathrm{d}t \geqslant 0, \tag{2.7}$$

remembering that, from physical reasons,

$$\int_0^{2\pi/\bar{\sigma}} \Xi_1(\cos(\bar{\sigma}t), -\sin(\bar{\sigma}t))\cos(\bar{\sigma}t)\,\mathrm{d}t = 0. \tag{2.8}$$

The steady-state analysis does not require to explicitly know $\Xi_1(\beta_1, \dot{\beta}_1)$. Any quadratic function Ξ_1 satisfying (2.7) and (2.8) is allowed. An appropriate expression of Ξ_1 for transient wave computations by (2.1) is discussed in § 4 Conclusions.

Taking the sum of squares in (2.5*a*,*b*) makes it possible to rewrite the secular system to the form

$$a^2[(m_1(\xi_2)a^2+(\hat{\sigma}^2-1))^2+(m_2(\xi_2)a^2-2\xi_1(1+\xi a))^2]=\epsilon^2, \tag{2.9a}$$

$$\theta=\mathrm{atan2}([m_2(\xi_2)a^2-2\xi_1(1+\xi a)],\quad [m_1(\xi_2)a^2+(\hat{\sigma}^2-1)]) \tag{2.9b}$$

(atan2(y, x) is the 2-argument arctangent) that can be solved to get an analytical prediction of the resonant response curves. Indeed, (2.9*a*) gives

$$\begin{aligned}\bar{\sigma}^{-2}(a;\xi_1,\xi_2,\xi,\epsilon)&=\hat{\sigma}^2(a;\xi_1,\xi_2,\xi,\epsilon)\\&=1-m_1(\xi_2)a^2\pm\sqrt{\frac{\epsilon^2}{a^2}-[m_2(\xi_2)a^2-2\xi_1(1+\xi a)]^2},\end{aligned} \tag{2.10}$$

which has the physical meaning when both the right-hand side and expression under the square root are non-negative that yields the left and right bounds in

$$a_{min}(\xi_1,\xi_2,\xi,\epsilon)\leqslant a\leqslant a_{max}(\xi_1,\xi_2,\xi,\epsilon). \tag{2.11}$$

Furthermore, inserting (2.10) into (2.9*b*) derives

$$\theta(a;\xi_1,\xi_2,\xi,\epsilon)=\mathrm{atan2}(m_2(\xi_2)a^2-2\xi_1(1+\xi a),m_1(\xi_2)a^2+(\hat{\sigma}^2(a;\xi_1,\xi_2,\xi,\epsilon)-1), \tag{2.12}$$

where $\hat{\sigma}^2$ should be taken from (2.10).

Hence, when varying a in the interval (2.11) for a fixed set of ξ_1, ξ_2, ξ and ϵ, (2.10) and (2.12) parametrically define the phase-lag response curve in the $(\bar{\sigma},\theta)$-plane but (2.10) as function of a determines the wave-amplitude response curve in the $(\bar{\sigma},a)$-plane.

3. Learning ξ_1, ξ_2 and ξ from measurements of the phase lag

The unknowns ξ_1, ξ_2 and ξ can be 'learnt' by using a set of the measurements of $\theta_i^{(n)}$ with the given $\bar{\sigma}_1^{(i,n)}$ and $\epsilon_n=P_1\eta_{2a}^{(n)}$, $n=1,\ldots,N_{\eta_{2a}}$. For this purpose, we introduce the distance function D between the phase-lag response curve by (2.10)–(2.12) and $(\bar{\sigma}_1^{(i,n)},\theta_i^{(n)})$ as

$$\begin{aligned}&D(n,i;\xi_1,\xi_2,\xi)\\&\quad=\sqrt{\min_{a_{min}\leqslant a\leqslant a_{max}}[(\bar{\sigma}(a;\xi_1,\xi_2,\xi,\epsilon_n)-\bar{\sigma}_1^{(i,n)})^2+(\theta(a;\xi_1,\xi_2,\xi,\epsilon_n)-\theta_i^{(n)})^2]};\end{aligned} \tag{3.1}$$

it depends on the indexes n and i enumerating $\bar{\sigma}_1^{(i,n)}$, $\theta_i^{(n)}$ and ϵ_n. Therefore, the integral distance

$$C(\xi_1,\xi_2,\xi)=\sum_{n=1}^{N_{\eta_{2a}}}\sum_i D(n,i;\xi_1,\xi_2,\xi)>0 \tag{3.2}$$

between all the adopted measurement points and asymptotic solution (2.10)–(2.12) may be taken as the loss function in the machine learning procedure. The wanted damping-related parameters ξ_1, ξ_2 and ξ realise the absolute minimum of the mean-square error-function C. Minimisation of the loss function (3.2) can be done by the gradient descent. The absolute minimum of C exists and, from geometrical and physical point of view, is unique. Hypothetically, if the absolute minimum is realised on a manifold in the (ξ_1,ξ_2,ξ)-space, standard gradient-descent algorithms should effectively detect it.

3.1. *Employing the measurements by Bäuerlein & Avila (2021)*

Experimental data on the liquid-mass centre (horizontal steady-state wave amplitude and phase lag) were reported by Bäuerlein & Avila (2021). Horizontal position of the liquid-mass centre is, according to Faltinsen & Timokha (2009, (8.73)), described by

$$y_C(t) = -\frac{2}{\pi^2 h}\beta_1(t) + O(a^3) = -\frac{2}{\pi^2 h} a\cos\bar{\sigma}t + O(a^3). \tag{3.3}$$

This means that the theoretical steady-state phase lag and wave amplitude in experiments by Bäuerlein & Avila (2021) could in the lowest-order approximation be associated with θ and $2a/(\pi^2 h)$ coming from the asymptotic solution (2.10)–(2.12).

The experimental model tests by Bäuerlein & Avila (2021) were done with the non-dimensional liquid depth $h = 0.8$ that implies (Faltinsen & Timokha 2009, table 9.1) $d_2 = 3.142$, $d_2 = 2.533$, $d_3 = -0.021$, $d_4 = -0.042$, $d_5 = -3.225$. The experimental forcing amplitudes were $\eta_{2a} = 0.0009$, 0.0017, 0.0032 and 0.0064. The low-viscous (fresh water) liquid with the kinematic viscosity $\nu = 10^{-6}$ m^2 s^{-1} is used. At the same time, visual observations with $\eta_{2a} = 0.0064$ discovered wave breaking, overturning and serious contribution of higher modes/harmonics that indicates inapplicability of the single-dominant modal theory for the experimental series with the largest excitation amplitude.

Utilising experimental series with $\eta_{2a} = 0.009$ (I), 0.0017 (II) and 0.0032 (III) in the above-proposed machine learning procedure makes it possible to compute ξ_1, ξ_2 and ξ. The theoretical accuracy should statistically depend on the accuracy of the measured data. Ideally, if all the measurements I + II + III are used for training, that computes $\xi_1 = \xi_1^l = 0.007167965$, $\xi_2 = \xi_2^l = 0.01002107$ and $\xi = \xi^l = 0.2636$. Other acceptable trainings were: I + III $\to$ 0.00710169946, 0.0095860284, 0.193322; I + II $\to$ 0.00733898346, 0.010288244, 0.0931; III $\to$ 0.0073849521, 0.005228571, 0.37915. Inserting these values into expressions (2.10)–(2.12) makes it possible to draw the theoretical phase-lag response curves to be compared with measurements adopted for both training and testing. Our numerical experiments showed that the training strategies III, I + II, I + III and I + II + III lead to visually almost identical curves. The triad $\xi_1 = \xi_1^l = 0.007167965$, $\xi_2 = \xi_2^l = 0.01002107$, $\xi = \xi^l = 0.2636$ with I + II + III is therefore adopted in the graphical analysis.

Figure 1(*a*) confirms applicability of the single-dominant modal theory (2.1). Agreement is excellent, especially, in contrast to Bäuerlein & Avila (2021, figure 14) who adopted $\xi_1 = \xi_1^{exp} = 8.4 \times 10^{-3}$ (coming from the measured logarithmic decrements) and $\xi_2 = \xi = 0$ in their computations by the single-dominant modal system. Agreement in figure 1(*a*) is also much better than with using the Duffing mathematical model by Bäuerlein & Avila (2021, figure 13). As matter of the fact, we showed that damping of the second-order mode (non-zero ξ_2 in (2.1*b*)) and the quadratic damping Ξ_1 in the first modal equation (2.1*a*) matter.

Even though, as we remarked above, the single-dominant modal theory is not applicable for the largest experimental forcing amplitude $\eta_{2a} = 0.0064$, the computed $\xi_1 = \xi_1^l$, $\xi_2 = \xi_2^l$, $\xi = \xi^l$ and $\epsilon = P_1\eta_{2a} = P_1 \times 0.0064$ were used in (2.10)–(2.12) to draw the theoretical phase-lag response curve and compare it with the corresponding measurements by Bäuerlein & Avila (2021). The numerical results are shown in figure 1(*b*). The figure detects a zone where the single-dominant modal theory is clearly non-applicable (wave breaking and other free-surface phenomena indeed matter!). Far from this zone, agreement between the learnt solution and experiments is also excellent.

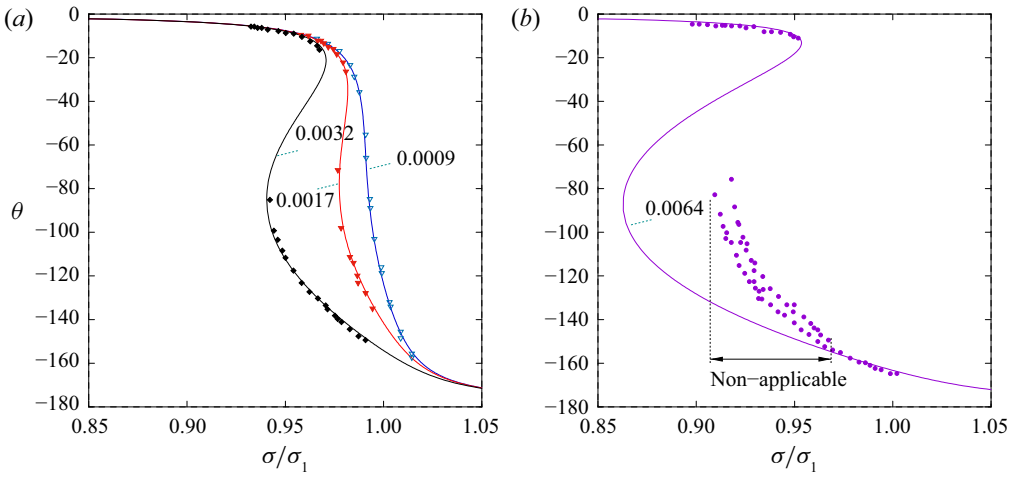

Figure 1. The theoretical (lines) and experimental (symbols) phase-lag (in grads) response curves for the experimental set-up by Bäuerlein & Avila (2021). The measured phase lags with the forcing amplitudes $\eta_{2a} = 0.0009$, 0.0017 and 0.0032 from the (a) were used in the machine learning procedure from § 3 to compute $\xi_1 = \xi_1^l = 0.007167965$, $\xi_2 = \xi_2^l = 0.01002107$ and $\xi = \xi^l = 0.2636$ and substitute them into (2.10)–(2.12). Panel (b) is drawn for the largest experimental forcing amplitude $\eta_{2a} = 0.0064$ when the single-dominant modal system is, generally, not applicable; it detects a zone where this happens.

We used asymptotic solution (2.10)–(2.12) with $\xi_1 = \xi_1^l = 0.007167965$, $\xi_2 = \xi_2^l = 0.01002107$ and $\xi = \xi^l = 0.2636$ to compare the theoretical mass-centre amplitude by (3.3) with measurements by Bäuerlein & Avila (2021). The results are presented in figure 2. Figure 2(a) is drawn for the cases from figure 1(a) but figure 2(b) corresponds to $\eta_{2a} = 0.0064$. The dashed lines in figure 2(a) imply the inviscid single-dominant theory for $\eta_{2a} = 0.0009$ and 0.0032.

Damping is responsible for the horizontal position of the jump-down bifurcation point P (demonstrated for the Duffing-type systems, e.g. by Faltinsen & Timokha 2009, § 8.2.1.3). As for the horizontal position of P, agreement between the 'learnt viscous' solution and measurements by Bäuerlein & Avila (2021) is rather good in figure 2(a) but the single-dominant theory is not applicable in the case in figure 2(b). Except in the left of P on the upper subbranch, discrepancy between theoretical viscous and inviscid amplitudes does not look dramatic for the larger forcing amplitude $\eta_{2a} = 0.0032$, whereas both theories are rather inaccurate to fit the measurements. The situation is opposite for the lowest tested forcing amplitude $\eta_{2a} = 0.0009$. The latter facts confirm earlier conclusions by Faltinsen & Timokha (2001) who showed for clean tanks that viscous damping may cause almost negligible effect on the wave amplitude with increasing excitation amplitude when, contrarily, the free-surface nonlinearity and associated energy flow between the generalised hydrodynamic coordinates (modes) play dominant roles. Faltinsen & Timokha (2001) showed that agreement for the wave-amplitude response curves with increasing forcing amplitude can be improved when using an adaptive modal theory with zero damping or small damping following from the single-dominant prediction.

3.2. *Linear damping ratios ξ_1 and ξ_2*

Neglecting nonlinear terms in (2.1) leads to an infinite set of linear oscillators, equations of the so-called linear modal theory by Faltinsen & Timokha (2009, chap. 5), which is

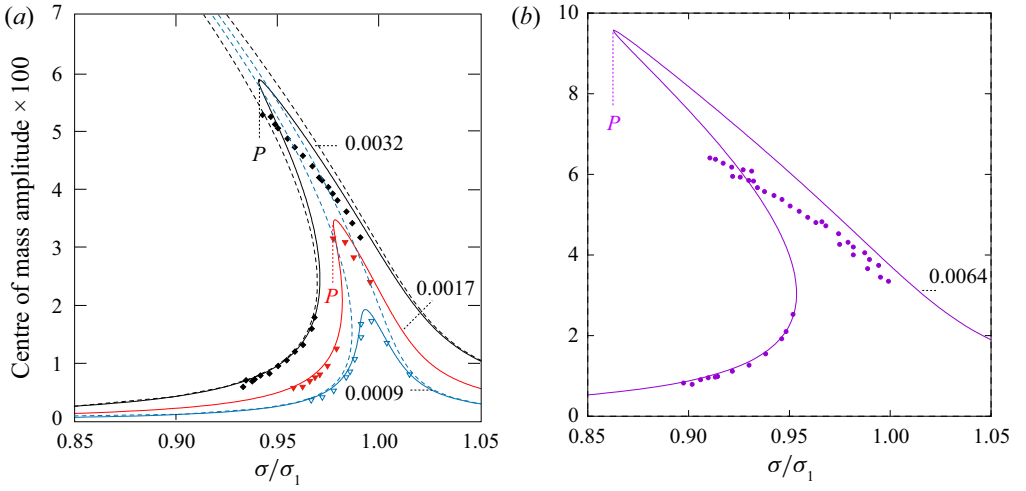

Figure 2. The same as in figure 1 but for the liquid-mass centre amplitude. The fully inviscid branching by the single-dominant theory is shown in (*a*) by the dashed lines for $\eta_{2a} = 0.0009$ and 0.0032 to confirm that it cannot predict horizontal position of the jump-down bifurcation point P, which is a function of viscous damping. For the smaller forcing, $\eta_{2a} = 0.0009$, discrepancy between viscous and inviscid theoretical amplitude near the amplitude peak is huge while, for the larger one, $\eta_{2a} = 0.0032$, it does not look dramatical.

applicable to non-resonant sloshing of a low-viscous liquid. When posing $\eta_{2a} = 0$, its solution determines a superposition of decaying standing Stokes waves whose logarithmic decrements are associated with the linear damping ratios ξ_i.

Rigorous linear mathematical theory of viscous unforced sloshing was created by Selim Krein (1964). Krein's theorem states that only a finite number of oscillatory sloshing modes exists, i.e. interpreting his result in terms of the linear modal theory with $\eta_{2a} = 0$, there exists N such that $\xi_i > \bar{\sigma}_i$ for $i \geqslant N$. Numerical analysis by Barnyak & Barnyak (1996) also shows that only lower sloshing modes and frequencies of viscous liquids can be approximated within the framework of the inviscid hydrodynamic theory. The inequality and computations are in conflict with assumptions of the linear damped modal theory, which requires small ξ_i to weakly affect the natural sloshing frequencies and modes, namely, the theory requires $\xi_i \ll \bar{\sigma}_i$ on an asymptotic scale. The latter can only be fulfilled for a few lower natural sloshing modes. Now, readers may understand why we postulated $O(\epsilon^{1/3}) = \xi_i \ll \bar{\sigma}_i = O(1)$ only for $i = 1, 2$ and 3.

When associating $\xi_i \ll 1$ with logarithmic decrements of lower natural sloshing modes, these can be estimated from below (Faltinsen & Timokha 2009, chap. 6) by using asymptotic formulas, which are based on the laminar boundary-layer theory for low-viscous liquids and accounting for the bulk damping effects, $\xi_i^{(0)} = \xi_i^{layer} + \xi_i^{bulk} \lesssim \xi_i$. Miles (1967), Miles & Henderson (1998) and Faltinsen & Timokha (2009, chap. 6) discussed why and when the bulk damping may matter as well as how other potentially valuable viscous mechanisms including the dynamic contact angle, wave breaking, free-surface contamination and roof impact can significantly increase the damping. Taking Keulegan's estimate for ξ_i^{layer} and (6.139) by Faltinsen & Timokha (2009) for ξ_i^{bulk} gives

$$\xi_i^{(0)} = \sqrt{\frac{\nu}{2\sigma_i}}\frac{1}{B}\left(1 + \frac{B}{L}\left[1 + \pi i \frac{1-2h}{\sinh(2\pi i h)}\right]\right) + 2\nu\frac{\pi^2 i^2}{L^2\sigma_i^2}, \tag{3.4}$$

where ν is the kinematic viscosity. Specifically, the formula provides $\xi_i^0/\bar{\sigma}_i \to \infty$ as $i \to \infty$ but, as we stated above, (3.4) is valid only for lower indices i and strongly requires $\xi_i^{(0)} \ll O(1)$.

For the experimental set-up by Bäuerlein & Avila (2021, $L = 0.5$ m, $B = 0.05$ m and $h = 0.8$) with fresh water, (3.4) outputs $\xi_1^{(0)} = 0.0057$ and $\xi_2^{(0)} = 0.0047$; the computed values are practically not affected by the bulk damping and, therefore, one can say that these imply the Keulegan's approximation. The Keulegan's damping ratios are definitely lower than $\xi_1^l = 0.007167965$ and $\xi_2^l = 0.01002107$ coming from the machine learning procedure with $\eta_{2a} = 0.0009$, 0.0017 and 0.0032. The inequality is correct because (3.4) estimates from below.

Bäuerlein & Avila (2021) conducted special model tests attempting to estimate ξ_1. They interrupted harmonic excitations of the steady-state wave with $\eta_{2a} = 0.0064$ at an instant $t = t_0$ and, thereafter, measured logarithmic decrements of the wave decay. The averaged experimental value of ξ_1 coming from the measured decrements was estimated at $\xi_1 = \xi_1^{exp} = 0.0084$. This value is larger than $\xi_1^l = 0.007167965$ because of, most probably, very specific free-surface phenomena discovered for model tests with $\eta_{2a} = 0.0064$ that could affect logarithmic decrements even after interrupting the harmonic forcing.

On the other hand, the theoretical linear damping rate of the second natural sloshing mode, $\xi_2^{(0)} = 0.0047$, is too low with respect to $\xi_2^l = 0.01002107$. The discrepancy between $\xi_2^{(0)}$ and ξ_2^l may be explained by an 'inaccurate' modelling of energy flow between the second and higher modes. The single-dominant modal theory simply ignores this. Using an adaptive modal system by Faltinsen & Timokha (2001) would lead to a more accurate distribution of ξ_i, $i \geqslant 2$ and improve agreement in figure 2(*a*). However, the adaptive modal systems do not have analytical solutions, that is, the machine learning procedure becomes then much more complicated.

4. Conclusions

Estimates of viscous damping in liquid sloshing dynamics can be done by applying a machine learning procedure to multimodal systems with unknown *a priori* viscous damping terms. Such a procedure was developed for the single-dominant modal system/theory by Faltinsen *et al.* (2000) when the steady-state wave (periodic) solution can analytically be derived by using Moiseev's asymptotic scheme. The solution becomes a function of three unknown parameters, ξ_1, ξ_2 and ξ, responsible for damping in the hydrodynamic system. Having known measurements of the phase lags makes it possible to compute (learn) these parameters. The measured phase lags by Bäuerlein & Avila (2021) are employed to evaluate abilities of the proposed procedure and find $\xi_1 = \xi_1^l$, $\xi_2 = \xi_2^l$ and $\xi = \xi^l$. An excellent agreement is demonstrated except when, according to visual observations in Bäuerlein & Avila (2021), the single-dominant system is not applicable. Following the physics-driven machine learning instead of the data-driven approach by Cenedese *et al.* (2022) did not provide good agreement for all the steady-state amplitude parameters but made it possible to make several physical conclusions on nonlinear sloshing. The obtained results can also be generalised to transient waves and coupling with tank motions, including in ship dynamics.

One conclusion is that effect of higher (here, second) natural sloshing modes (nonlinear energy transfer from the primary-excited to the higher modes) and viscous damping of these modes cannot be neglected. Furthermore, viscous damping of the primary-excited (first) natural sloshing mode should, generally speaking, be a function of the wave

amplitude and, moreover, for the single-dominant system, the function is just the linear regression. Finally, the proposed procedure can be an efficient tool for estimating the viscous damping of the lowest (dominant) natural sloshing mode, but it fails for the higher (order) modes. To get more accurate ξ_2, one should use an adaptive multimodal system by Faltinsen & Timokha (2001) where $\beta_1 \sim \beta_2$. Such a system is also required for an accurate prediction of the wave-amplitude response curves.

Derivations of the steady-state wave (periodic) solution does not require an exact analytical expression for $\Xi_1(\beta_1, \dot{\beta}_1)$. Any analytical quadratic form of Ξ_1 is allowed if it deduces the two integrals (2.7) and (2.8). An example could be

$$\Xi_1(\beta_1, \dot{\beta}_1) = \xi \frac{3\pi}{8} |\dot{\beta}_1| \, \dot{\beta}_1, \tag{4.1}$$

which physically implies a drag force. Based on model tests by Faltinsen *et al.* (2000) and other authors with transient waves, one should check whether (4.1) is indeed applicable.

Funding. A.T. acknowledges financial support of the National Research Foundation of Ukraine (project number 2020.02/0089).

Declaration of interests. The authors report no conflict of interest.

Author ORCIDs.
Alexander Timokha https://orcid.org/0000-0002-6750-4727.

References

Ahmed, S.E., Pawar, S., San, O., Rasheed, A., Iliescu, T. & Noack, D. 2021 On closures for reduced order models – a spectrum of first-principle to machine–learned avenues. *Phys. Fluids* **33** (9), 091301.

Aliabadi, S., Johnson, A. & Abedi, J. 2003 Comparison of finite element and pendulum models for simulating of sloshing. *Comput. Fluids* **32**, 535–545.

Barnyak, M.Y. & Barnyak, O.M. 1996 Normal oscillations of viscous liquid in a horizontal channel. *Intl Appl. Mech.* **32** (7), 56–566.

Bäuerlein, B. & Avila, K. 2021 Phase lag predicts nonlinear response maxima in liquid-sloshing experiments. *J. Fluid Mech.* **925**, A22.

Cenedese, M., Axås, J., Bäuerlein, B., Avila, K. & Haller, G. 2022 Data-driven modeling and prediction of non-linearizable dynamics via spectral submanifolds. *Nat. Commun.* **13**, 872.

Faltinsen, O.M. 1974 A nonlinear theory of sloshing in rectangular tanks. *J. Ship Res.* **18**, 224–241.

Faltinsen, O.M., Rognebakke, O.F., Lukovsky, I.A. & Timokha, A.N. 2000 Multidimensional modal analysis of nonlinear sloshing in a rectangular tank with finite water depth. *J. Fluid Mech.* **407**, 201–234.

Faltinsen, O.M. & Timokha, A.N. 2001 Adaptive multimodal approach to nonlinear sloshing in a rectangular tank. *J. Fluid Mech.* **432**, 167–200.

Faltinsen, O.M. & Timokha, A.N. 2009 *Sloshing*. Cambridge University Press.

Godderidge, B., Turnock, S.R. & Tan, M. 2012 A rapid method for the simulation of sloshing using a mathematical model based on the pendulum equation. *Comput. Fluids* **57**, 163–171.

Keulegan, G. 1959 Energy dissipation in standing waves in rectangular basins. *J. Fluid Mech.* **6** (1), 33–50.

Krein, S.G. 1964 Oscillations of a viscous fluid in a container (in Russian). *Dokl. Akad. Nauk SSSR* **159**, 262–265.

Miles, J.W. 1962 Stability of forced oscillations of a spherical pendulum. *Q. Appl. Maths* **20** (1), 21–32.

Miles, J.W. 1967 Surface-wave damping in closed basins. *Proc. R. Soc. Lond.* A **A297**, 459–475.

Miles, J.W. & Henderson, D.M. 1998 A note on interior vs boundary-layer damping of surface waves in a cicular cylinder. *J. Fluid Mech.* **364**, 319–323.

NASA 1968 Propellant slosh loads. *Tech. Rep.* NASA SP-8009.

Ockendon, J.R. & Ockendon, H. 1973 Resonant surface waves. *J. Fluid Mech.* **59**, 397–413.

Pilipchuk, V.N. 2013 Nonlinear interactions and energy exchange between liquid sloshing modes. *Physica* D **263**, 21–40.

Raissi, M. & Karniadakis, G.E. 2018 Hidden physics models: machine learning of nonlinear partial differential equations. *J. Comput. Phys.* **357**, 125–141.

RAISSI, M., PERDIKARIS, P. & KARNIADAKIS, G.E. 2019 Physics-informed neural networks: a deep learning framework for solving forward and inverse problems involving nonlinear partial differential equations. *J. Comput. Phys.* **378**, 686–707.

SALTARI, F., PIZZOLI, M., COPPOTELLI, G., GAMBIOLI, F., COOPER, J.F. & MASTRODDI, F. 2022 Experimental characterisation of sloshing tank dissipative behaviour in vertical harmonic excitation. *J. Fluids Struct.* **109**, 103478.